

Supraglacial Streams on the Greenland Ice Sheet Delineated From Combined Spectral–Shape Information in High-Resolution Satellite Imagery

Kang Yang and Laurence C. Smith

Abstract—Supraglacial meltwater streams and lakes that form each summer across large expanses of the Greenland Ice Sheet (GrIS) ablation zone have global implications for sea level rise but remain one of the least studied hydrologic systems on Earth. Remote sensing of supraglacial streams is challenging owing to their narrow width ($\sim 1\text{--}30$ m) and proximity to other features having similar visible/near-infrared reflectance (lakes and slush) or shape (dry stream channels, crevasses, and fractures). This letter presents a new automated “spectral–shape” procedure for delineating actively flowing streams in high-resolution satellite imagery, utilizing both spectral and pattern information. First, a modified normalized difference water index adapted for ice (NDWI_{ice}) enhances the spectral contrast between open water and drier snow/ice surfaces. Next, three NDWI_{ice} thresholds are used to mask deep-water lakes and discern open water from slush, in concert with a multipoints fast marching method to rejoin resulting stream fragments. Comparison of this procedure with manual digitization for six WorldView-2 images in southwestern Greenland demonstrates its value for detecting actively flowing supraglacial streams, particularly in slushy areas where classification performance dramatically improves (85.2% success) versus simple threshold methods (52.9% and 59.4% success for low and moderate thresholds, respectively). While a simple threshold approach is satisfactory for areas known to be slush free, the procedure outlined here enables comprehensive stream mapping across the GrIS ablation zone, regardless of slush conditions and/or the presence of similarly shaped glaciological features.

Index Terms—Fast marching method, Greenland Ice Sheet (GrIS), mathematical morphology, normalized difference water index (NDWI), supraglacial stream hydrology, WorldView-2.

I. INTRODUCTION

THE Greenland Ice Sheet (GrIS) is losing mass due to a combination of increased surface meltwater runoff and iceberg calving [1], [2]. Estimates of the former are large and have been calculated to contribute more than $\sim 40\%$ of the total GrIS mass loss from 2000 to 2008 [3]. However,

Manuscript received June 13, 2012; revised August 28, 2012; accepted September 28, 2012. Date of publication November 26, 2012; date of current version April 4, 2013. This work was supported by the NASA Cryosphere Program under Grant NNX11AQ38G and a fellowship from China Scholarship Council.

K. Yang is with the Department of Geographic Information Science, Nanjing University, Nanjing 210093, China (e-mail: yangkangnju@gmail.com).

L. C. Smith is with the Department of Geography, University of California, Los Angeles, CA 90095 USA (e-mail: lsmith@geog.ucla.edu).

Color versions of one or more of the figures in this paper are available online at <http://ieeexplore.ieee.org>.

Digital Object Identifier 10.1109/LGRS.2012.2224316

such estimates remain unverified because they are derived from climate variables and modeling, rather than direct observations of hydrologic processes on the ice sheet.

One reason for this is that the GrIS surface drainage system is extraordinarily complex, consisting of a largely unstudied ephemeral patchwork of supraglacial lakes, streams, crevasses, fractures, and moulins (vertical conduits that conduct water to the subsurface) [4]. High-resolution mapping of these features and their evolution over time would substantially advance scientific understanding of GrIS mass balance, ice flow dynamics, and contributions to global sea level rise. However, most remote-sensing studies of GrIS supraglacial hydrology to date have focused on the distribution and evolution of lakes large enough to be visible in coarse- or moderate- resolution satellite imagery (e.g., Moderate Resolution Imaging Spectroradiometer, Landsat Thematic Mapper/Enhanced Thematic Mapper Plus, and Advanced Spaceborne Thermal Emission and Reflection Radiometer [5]–[12]). Aside from field studies [13], [14], far less attention has been given to supraglacial streams; thus, even basic understanding of their abundance, temporal dynamics, and interactions with glaciological features is currently lacking [15].

A prime reason for this knowledge gap is that flow widths of most supraglacial streams are too narrow ($\sim 1\text{--}30$ m) to be confidently detected in coarse- or moderate-resolution satellite imagery. However, a growing availability of high-resolution imagery such as IKONOS, GeoEye, QuickBird, and WorldView-1/2 raises prospects for studying the evolution of supraglacial stream networks across the GrIS. This requires new automated computational methods to be developed, owing to the large number of images required to study hydrologic processes with high spatial resolution across large areas of the ablation zone. A particular challenge is discriminating actively flowing supraglacial streams from other glaciological features with similar spectral signatures (particularly slush, which often has low visible/near-infrared (NIR) reflectance such as open water), and shapes (e.g., dry stream channels, crevasses, and fractures) also common to the ablation zone of the GrIS.

This letter presents an automated procedure to exploit both spectral and shape information to delineate supraglacial streams on the GrIS ablation zone using high-resolution visible/NIR satellite imagery. Its overall strategy is to use both spectral and shape information to discern actively flowing streams from other features with similar visible/NIR reflectance

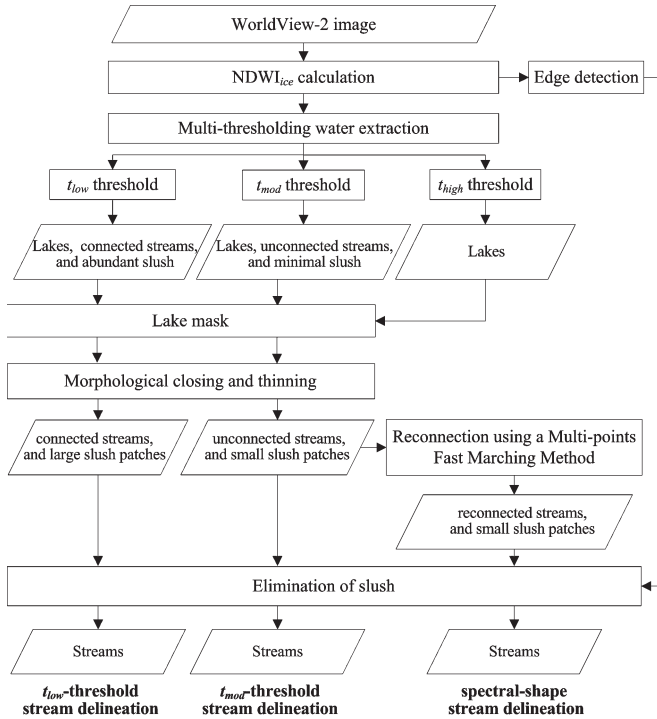


Fig. 1. Methodological flowchart for delineating actively flowing supraglacial streams on the GrIS.

(e.g., lakes and slush) and/or shape (dry stream channels, crevasses, and fractures). Therefore, its prime tasks are as follows: 1) distinguish active streams from lakes, slush and ice; 2) distinguish active streams from other linear and/or semilinear features that do not contain water; and 3) test and validate this approach using WorldView-2 imagery acquired for the GrIS ablation zone near Kangerlussuaq, southwestern Greenland, an area rich in supraglacial stream networks. These tasks are achieved through a multistep procedure of water extraction, stream delineation, and slush elimination (see Fig. 1) as follows.

II. METHODOLOGY

A. Water Extraction

The first step is to extract all wet features (flowing streams, lakes, and slush) present on the ice sheet through spectral discrimination from bare ice, dry snow, and firn. This was achieved through modification of the normalized difference water index (NDWI), which is usually used for delineation of open water on terrestrial land surfaces [16]. NDWI is typically calculated using the normalized ratio of green and NIR bands ($NDWI = (GREEN - NIR)/(GREEN + NIR)$), owing to higher NIR reflectance of surrounding terrestrial vegetation and soil relative to water. However, this approach is unsuitable for glaciological environments as melting ice, snow, and firn also have low reflectivity in the NIR wavelengths. The modified NDWI proposed here instead uses the normalized ratio of the blue and red bands to better discern supraglacial water features in this unique environment, i.e.,

$$NDWI_{ice} = \frac{BLUE - RED}{BLUE + RED}. \quad (1)$$

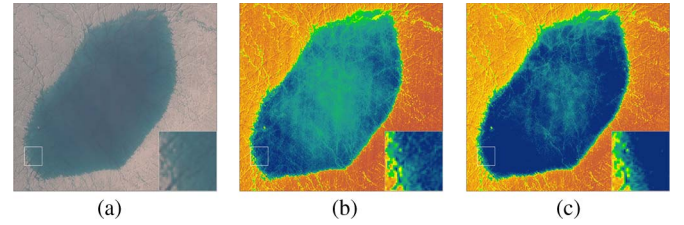


Fig. 2. Two NDWI transformations of a GrIS supraglacial lake. (a) WorldView-2 image (red, green, and blue (RGB): bands 5, 3, and 2). (b) Conventional NDWI. (c) Ice-adapted $NDWI_{ice}$.

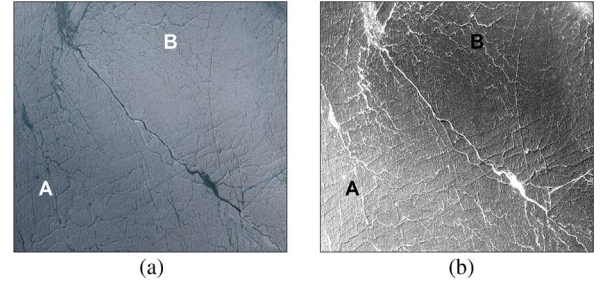


Fig. 3. WorldView-2 and $NDWI_{ice}$ images of supraglacial stream networks. (a) WorldView-2 image (RGB: bands 5, 3, and 2) containing numerous supraglacial streams in both a slush region (A) and a nonslush region (B). (b) Corresponding $NDWI_{ice}$ image revealing higher $NDWI_{ice}$ values in slush.

This $NDWI_{ice}$ is particularly suitable for use with WorldView-2 imagery, owing to fairly strong water/ice contrast in the red band (630–690 nm) and relatively high reflectance of water in the blue band (450–510 nm). For example, a comparison of conventional NDWI and $NDWI_{ice}$ retrievals for a GrIS supraglacial lake reveals a more clearly defined lake boundary and homogenous lake interior for $NDWI_{ice}$ (see Fig. 2). $NDWI_{ice}$ was therefore used as the basis for all further water delineations in this study.

Ideally, one global $NDWI_{ice}$ threshold would classify each image into either “water” or “nonwater” regions. This is confounded on the GrIS by the presence of slush (wet or saturated snow and/or firn). Slush is a common transitional material in the GrIS ablation zone often found alongside liquid water and bare ice, usually in areas of low relief [see Fig. 3(a)]. Owing to its high liquid water content, slush often has similarly low visible/NIR spectral reflectance as supraglacial streams, thus presenting an important challenge for distinguishing these two materials. As a result, $NDWI_{ice}$ only partially discerns slush from liquid water and may completely fail in very wet and/or saturated areas.

Although $NDWI_{ice}$ values for slush are lower than values for lakes, they commonly have even higher $NDWI_{ice}$ values than actively flowing streams [see Fig. 3(b)]. Therefore, a single global threshold is insufficient for universal stream detection, and a multithreshold method [9] is developed here. In total, three global thresholds were used: 1) a liberal $NDWI_{ice}$ threshold designed to capture as many “water” pixels as possible (t_{low}); 2) a stringent $NDWI_{ice}$ threshold designed to capture deep-water bodies such as lakes (t_{high}); and 3) an intermediate $NDWI_{ice}$ value (t_{mod}) between t_{low} and t_{high} designed to help eliminate slush. The criterion of threshold determination is as follows: t_{low} is determined by averaging the $NDWI_{ice}$ values

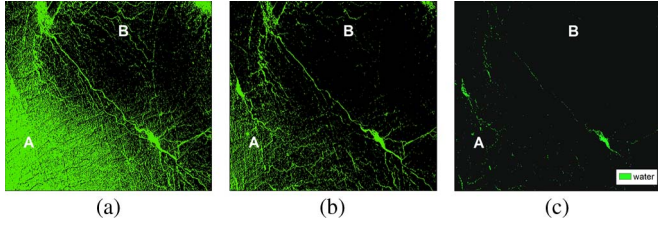


Fig. 4. Global “water” classifications using three $NDWI_{ice}$ thresholds. (a) t_{low} . (b) t_{mod} . (c) t_{high} .

of randomly selected pixels from ten “small” stream segments (1 pixel wide) that are visually recognizable throughout the image; t_{mod} is determined in a similar way, except the $NDWI_{ice}$ values are randomly selected from ten “large” streams (width > 1 pixel) throughout the image; and t_{high} is determined by averaging $NDWI_{ice}$ values from ten lakes throughout the image. In general, the $NDWI_{ice}$ values of streams and lakes were relatively uniform throughout the image. Applied universally, each threshold discerns supraglacial stream networks from slush to varying degrees of success, with a low threshold t_{low} , capturing excessive slush but preserving stream network continuity, the high threshold excluding all slush but capturing few streams, and the moderate threshold excluding most slush but also fragmenting the stream network (see Fig. 4).

B. Stream Delineation

Of the three $NDWI_{ice}$ thresholds, features extracted using t_{mod} were preferred for active stream delineation, owing to their capability to identify numerous active streams while eliminating most areas of slush. However, two issues still remained. First, not all slush was removed from the classification. Second, owing to longitudinal variations in $NDWI_{ice}$, this intermediate threshold sometimes failed to detect short segments along a stream course, causing gaps/disconnects in its corresponding delineation. The first problem was mitigated using an edge-detection method and is presented in Section II-C. The second problem was mitigated using the multipoints fast marching method [17], which is a novel variant of the fast marching method [18] as follows.

Given an image $I : \Omega \rightarrow \mathbb{R}^+$ and a source point list p_i ($i = 1, 2, \dots, N$), a cost surface $P : \Omega \rightarrow \mathbb{R}^+$ is built, which seeks lower values near desired features of the image. Propagations are simultaneously conducted from all the source points with propagation constraints (e.g., a neighborhood searching condition) as follows: 1) propagate and compute a minimal action map U_i to p_i ($i = 1, 2, \dots, N$) until no further valid propagation points are found, then record all the meeting points, and U_i could be regarded as the arrival time of a front propagating from the source p_i with cost P or velocity $1/P$; 2) select the meeting point p_{ij} with the lowest value of minimal action as the valid meeting point between the source point p_i and p_j ; 3) compute the minimal path between p_{ij} and p_i (p_j) through back propagation (gradient descent) from p_{ij} back to p_i (p_j) on U_i (U_j), respectively, to yield the two minimal paths, then join them to obtain the optimal minimal path between p_i and p_j ; and, finally, 4) compute the possible minimal paths between all source points in the image.

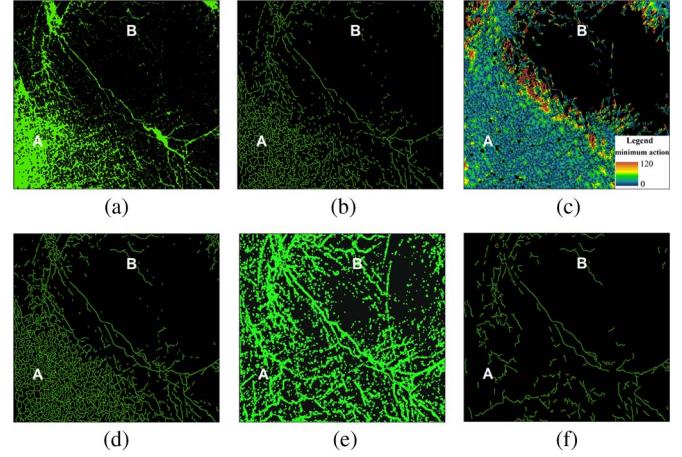


Fig. 5. Application of the spectral-shape method to the $NDWI_{ice}$ t_{mod} classification shown in Fig. 4(b). (a) Morphological closing. (b) Morphological thinning. (c) Minimal action map generated from the multipoints fast marching method. (d) Preliminary stream delineation with gaps rejoined. (e) Dilated edges from the Canny edge detector used to mask (d). (f) Final actively flowing supraglacial stream network after secondary slush elimination using edge detection.

To preprocess the t_{mod} $NDWI_{ice}$ mask for the multipoints fast marching method, a morphological closing operation (3×3 moving window) is used to fill missing water pixels or remove isolated ones [see Fig. 5(a)]. A morphological thinning operation (3×3 moving window) is then used to reduce water regions to 1-pixel-wide skeletal remnants in order to enable the multipoints fast marching method (and vectorization, if desired later) [see Fig. 5(b)]. These thinned water features are labeled “stream candidates” and rejoined using the multipoints fast marching method, with their endpoints being the source points of propagation and the $NDWI_{ice}$ inverse image the cost surface P (in which stream candidates have faster propagation velocities, i.e., low cost). This drives faster propagation between stream candidate endpoints, thus closing the gaps and producing the optimal (least cost) paths between them [see Fig. 5(c) and (d)].

Appropriate connection constraints are necessary since some linear or semilinear features on the ice sheet (e.g., dry stream channels, crevasses, and fractures) should be ignored. Note that the minimal action path of a source point is determined not only by its front propagation velocity but also by its distance to the other source points. Therefore, if the gap between two stream candidates is large, erroneous shortcuts (such as dry stream channels) may be obtained. To reduce this problem, a propagation constraint was implemented through a neighborhood searching condition. At each propagation step, the current point with the smallest action was selected, and only its neighbors with $NDWI_{ice}$ values greater than t_{low} were updated. This prevented dry stream channels from becoming connected because their $NDWI_{ice}$ values were almost always smaller than t_{low} , thus eliminating them from consideration as valid propagation points.

C. Slush Elimination

Even after stream delineation, some areas of slush still remained, some with actively flowing streams and some not

[see Fig. 5(d)]. These latter erroneous stream candidates were difficult to eliminate owing to their similar spectral characteristics with open water. This led to development of a shape-orientated approach to reduce erroneously thinned slush features while preserving active streams. The motivation for this approach is separation of low-reflectance actively flowing stream channels, which possess linear, crenulate, or sinuous shapes with high length/width ratios, from low reflectance slush areas, which do not. The dilated edge of the raw $NDWI_{ice}$ image was obtained by a Canny edge detector [19] and a morphological dilation operator (3×3 moving window), in which edges (active streams) were delineated while nonedges (erroneous slush features) were not [see Fig. 5(e)].

Only the pixels that were delineated in both the dilated edge image and the connected stream candidate image were marked as active stream pixels. The erroneously thinned features located in slush were thus removed if they did not overlay with edges. Importantly, the thresholds for the Canny edge detector were kept relatively low (35–45 for low threshold and 55–65 for high threshold based on the Canny edge detector output ranging from 0 to 255) to keep stream shapes complete because the nonstream edges will later be eliminated by overlaying a candidate connected stream image. A minimal size constraint P_{size} was imposed to remove small segments orphaned by the cutting effect of the dilation edge. Remaining stream candidates that survived all of these tests were encoded as “actively flowing streams” in the final product [see Fig. 5(f)].

III. EXPERIMENTAL RESULTS

Supraglacial stream delineations were carried out using the described “spectral–shape” method for six multispectral WorldView-2 images acquired on June 23, 2011 over the southwestern GrIS ablation zone near Kangerlussuaq. All coding was implemented using C# for Visual Studio. Optimal values for t_{low} , t_{mod} , and t_{high} were determined as 0.120, 0.140, and 0.250, respectively, through random selection of 10 pixels each from ten small stream segments (1 pixel wide), ten large stream segments (width > 1 pixel), and ten lakes, respectively, with standard deviations of 0.011, 0.008, and 0.021, respectively. A P_{size} setting of 5 pixels was used to remove short segments. For the Canny detector, values of 40 and 60 were used for the high and low edge thresholds, respectively.

To assess the performance of the automated stream delineations, six test sites ranging from 1.7 to 9.3 km² were selected (see Fig. 6), consisting of slush (sites 1–3) and nonslush (sites 4–6) stream-rich regions. For each site, independently derived stream delineations were manually digitized from false-color composites of the original WorldView-2 imagery, for comparison with the automated results. Performance accuracy was computed as the ratio of algorithm-derived stream pixels to manually digitized stream pixels.

For all six images, supraglacial streams were distinguished from slush, dry stream channels/crevasses/fractures, with good success, with 62 682 actively flowing streams identified (see Fig. 6). Within the validation test sites, the performance accuracy of the described spectral–shape method was 85.2%, as compared with 52.9% and 59.4%, respectively, using a

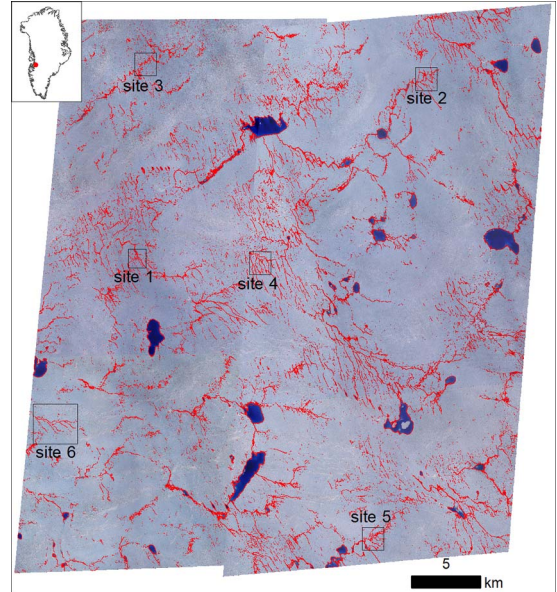


Fig. 6. Actively flowing supraglacial streams delineated from six WorldView-2 images of the GrIS ablation zone near Kangerlussuaq, southwestern Greenland, using the described spectral–shape method. Locations of six test sites manually digitized to assess performance accuracy (see Table I and Figs. 7 and 8) are also shown.

TABLE I
PERFORMANCE ACCURACY OF THE t_{low} -THRESHOLD, t_{mod} -THRESHOLD, AND SPECTRAL–SHAPE METHOD, AS COMPARED WITH MANUAL DIGITIZATION FOR THE SIX TEST SITES SHOWN IN FIG. 6

		t_{low} - threshold (%)	t_{mod} - threshold (%)	Spectral- shape (%)
Slush region	site 1	14.4	63.5	86.0
	site 2	13.0	64.1	95.0
	site 3	13.9	55.1	81.6
	Average (1-3)	13.8	60.9	87.6
Non- slush region	site 4	92.4	58.5	78.0
	site 5	94.3	65.3	87.6
	site 6	89.6	49.6	82.8
	Average (4-6)	92.1	57.8	82.8
	Average (1-6)	52.9	59.4	85.2

simple t_{low} - or t_{mod} -threshold alone (see Table I). In addition, the method identified 92 ponds and lakes, often connected to streams, thus revealing a complex supraglacial drainage system. In nonslush regions, however, a simple t_{low} -threshold offers an average accuracy value of 92.1% because this low threshold maintains stream network connectivity well in the absence of slush [see Fig. 8(c)]. This outperforms the spectral–shape method slightly (82.8%), suggesting a simple t_{low} -threshold is sufficient for stream delineation for those areas and/or times of year where slush is known to be absent on the ice sheet surface.

Because slush has high $NDWI_{ice}$ values and t_{low} cannot distinguish between slush and streams, the average performance accuracy of using the t_{low} -threshold alone to classify streams for sites 1–3 is only 13.8%, indicating that simple thresholding should not be applied to slushy regions [see Fig. 7(c)]. An intermediate t_{mod} -threshold results in high stream losses in both slush and nonslush regions [see Figs. 7(d) and 8(d)]

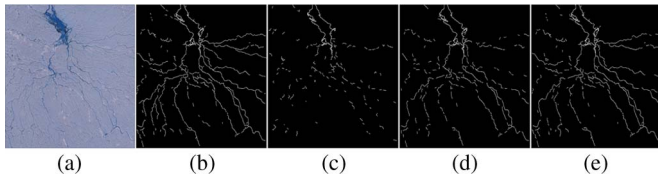


Fig. 7. Supraglacial stream delineations for test site 1 (slush region). (a) Raw WorldView-2 image. (b) Manually digitized stream network. (c) Delineation based on t_{low} only. (d) Delineation based on t_{mod} only. (e) Delineation based on t_{mod} , t_{low} , and shape information (spectral-shape method).

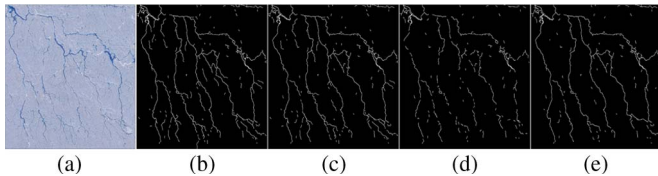


Fig. 8. Supraglacial stream delineations for test site 4 (non-slush region). (a) Raw WorldView-2 image. (b) Manually digitized stream network. (c) Delineation based on t_{low} only. (d) Delineation based on t_{mod} only. (e) Delineation based on t_{mod} , t_{low} , and shape information (spectral-shape method).

with an average accuracy value of 59.4% for the six regions, suggesting that a moderate threshold alone also does not yield accurate stream delineation. However, by incorporating both shape information and the additional t_{low} threshold as a reconnection constraint, its average performance accuracy improves to 85.2% [see Figs. 7(e) and 8(e)]. Finally, the spectral-shape stream delineation method shows high positional accuracy. The average position offset between delineated and manually digitized streams is within 1 pixel (~ 2.2 m). The maximal offset is about 2 pixels (~ 4.4 m), which occurred for some very wide streams (> 15 m) with high sinuosity, degrading accurate retrieval of their skeletal remnants.

IV. CONCLUDING REMARKS

The spectral-shape stream delineation procedure presented here has several areas for improvement. While edge detection eliminates centerlines from slush regions, it also eliminates small portions of active streams with diffuse edges. In addition, the multipoints fast marching method treats all streams with $NDWI_{ice}$ values smaller than t_{low} as dry stream channels, which is not always the case on the GrIS. Use of adaptive (rather than fixed) thresholds could mitigate this in the future.

Further research is also needed to improve edge detection in slush, construct topological and geomorphic relationships (such as drainage density and pattern, sinuosity, and stream order) from delineated stream networks, and test the procedure's application during other times of year and for other areas of the ice sheet.

Supraglacial streams are a crucial and little-studied component of the GrIS hydrologic drainage system but are challenging to delineate in visible/NIR imagery. This new combined spectral-shape method yields effective delineation of actively flowing streams while eliminating slush area with similar spectral signatures, as well as dry channels/crevasses/fractures with similar shapes. By fusing multithreshold and morphological

procedures with the use of edge detection, these difficulties are substantially overcome.

ACKNOWLEDGMENT

The authors would like to thank V. W. Chu, C. J. Gleason, and two anonymous reviewers for their detailed and constructive comments on this manuscript. WorldView-2 imagery was obtained through the Polar Geospatial Center, University of Minnesota.

REFERENCES

- [1] H. J. Zwally, W. Abdalati, T. Herring, K. Larson, J. Saba, and K. Steffen, "Surface melt-induced acceleration of Greenland Ice-Sheet flow," *Science*, vol. 297, no. 5579, pp. 218–222, Jul. 2002.
- [2] J. A. Dowdeswell, "The Greenland Ice Sheet and global sea-level rise," *Science*, vol. 311, no. 5763, pp. 963–964, Feb. 2006.
- [3] M. Van den Broeke, J. Bamber, J. Ettema, E. Rignot, E. Schrama, W. J. van de Berg, E. van Meijgaard, I. Velicogna, and B. Wouters, "Partitioning recent Greenland mass loss," *Science*, vol. 326, no. 5955, pp. 984–986, Nov. 2009.
- [4] T. Phillips, S. Leyk, H. Rajaram, W. Colgan, W. Abdalati, D. McGrath, and K. Steffen, "Modeling moulin distribution on Sermeq Avannarleq glacier using ASTER and WorldView imagery and fuzzy set theory," *Remote Sens. Environ.*, vol. 115, no. 9, pp. 2292–2301, Sep. 2011.
- [5] J. E. S. Box and K. Ski, "Remote sounding of Greenland supraglacial melt lakes: Implications for subglacial hydraulics," *J. Glaciol.*, vol. 53, no. 181, pp. 257–265, 2007.
- [6] M. McMillan, P. Nienow, A. Shepherd, T. Benham, and A. Sole, "Seasonal evolution of supra-glacial lakes on the Greenland Ice Sheet," *Earth Planet Sci. Lett.*, vol. 262, no. 3/4, pp. 484–492, Oct. 2007.
- [7] W. A. Sneed and G. S. Hamilton, "Evolution of melt pond volume on the surface of the Greenland Ice Sheet," *Geophys. Res. Lett.*, vol. 34, p. L03501, Feb. 2007.
- [8] S. Georgiou, A. Shepherd, M. McMillan, and P. Nienow, "Seasonal evolution of supraglacial lake volume from ASTER imagery," *Ann. Glaciol.*, vol. 50, no. 52, pp. 95–100, Oct. 2009.
- [9] A. V. Sundal, A. Shepherd, P. Nienow, E. Hanna, S. Palmer, and P. Huybrechts, "Evolution of supra-glacial lakes across the Greenland Ice Sheet," *Remote Sens. Environ.*, vol. 113, no. 10, pp. 2164–2171, Oct. 2009.
- [10] A. V. Sundal, A. Shepherd, P. Nienow, E. Hanna, S. Palmer, and P. Huybrechts, "Melt-induced speed-up of Greenland Ice Sheet offset by efficient subglacial drainage," *Nature*, vol. 469, no. 7331, pp. 521–524, Jan. 2011.
- [11] N. Selmes, T. Murray, and T. D. James, "Fast draining lakes on the Greenland Ice Sheet," *Geophys. Res. Lett.*, vol. 38, p. L15501, Aug. 2011.
- [12] Y. L. Liang, W. Colgan, Q. Lv, K. Steffen, W. Abdalati, J. Stroeve, D. Gallaher, and N. Bayou, "A decadal investigation of supraglacial lakes in West Greenland using a fully automatic detection and tracking algorithm," *Remote Sens. Environ.*, vol. 123, pp. 127–138, Aug. 2012.
- [13] G. A. Catania and T. A. Neumann, "Persistent englacial drainage features in the Greenland Ice Sheet," *Geophys. Res. Lett.*, vol. 37, p. L02501, Jan. 2010.
- [14] M. J. Hoffman, G. A. Catania, T. A. Neumann, L. C. Andrews, and J. A. Rumrill, "Links between acceleration, melting, and supraglacial lake drainage of the western Greenland Ice Sheet," *J. Geophys. Res.*, vol. 116, p. F04035, Dec. 2011.
- [15] T. D. L. Irvine-Fynn, A. J. Hodson, B. J. Moorman, G. Vatne, and A. L. Hubbard, "Polythermal glacier hydrology: A review," *Rev. Geophys.*, vol. 49, p. RG4002, Nov. 2011.
- [16] S. K. McFeeters, "The use of the normalized difference water index (NDWI) in the delineation of open water features," *Int. J. Remote Sens.*, vol. 17, no. 7, pp. 1425–1432, May 1996.
- [17] K. Yang, M. C. Li, Y. X. Liu, and C. Y. Jiang, "Multi-points fast marching: A novel method for road extraction," presented at the 2010 18th Int. Conf. Geoinformatics, Jun. 2010.
- [18] J. A. Sethian, "Evolution, implementation, and application of level set and fast marching methods for advancing fronts," *J. Comput. Phys.*, vol. 169, no. 2, pp. 503–555, May 2001.
- [19] J. Canny, "A computational approach to edge detection," *IEEE Trans. Pattern Anal.*, vol. PAMI-8, no. 6, pp. 679–698, Nov. 1986.